

INFLUENCE OF STACKING SEQUENCE ON THE IMPACT AND POSTIMPACT BENDING BEHAVIOR OF HYBRID SANDWICH COMPOSITES

M. Özen*

Keywords: hybrid sandwich composites, impact behavior, postimpact bending behavior, stacking sequence, VARIM.

A new hybrid sandwich structure was developed by using carbon, e-glass, and s-glass fabrics as reinforcement materials, an epoxy resin as the matrix material for face sheets, and a PVC foam as the core material. Six different configurations were prepared. Sandwich composites plates with different stacking sequences were subjected to low-speed impacts with energies of 7.5, 15, and 22.5 J. Their impact response is analyzed and reported in terms of the peak load as a function of impact energy. After impact tests, 3-point bending tests were conducted to determine the bending behavior of the sandwich composites after impacts in terms of their flexural strength. The results obtained showed that the use of carbon fabrics in the face sheets increased the peak loads for all the impact energies considered. The presence of carbon fibers in skin regions increased the flexural strength of the composites, but e-glass fibers decreased this strength.

Introduction

In the last few decades, there has been an increasing interest in using structural sandwich composite panels with various reinforced composite face sheets for a number of applications including aerospace, marine, wind turbines, buildings and transportations, owing to their good properties, such as a low weight, a superior bending stiffness, and ability to absorb impact energy. Many researchers have studied the failure mechanisms of sandwich structures under various static and dynamic loads, e.g., impacts [1-4].

Harran University, Engineering Faculty, Department of Mechanical Engineering, 63190 Osmanbey-Sanlıurfa, Turkey
*Corresponding author; tel.: +904143183000, +904143183799; e-mail: mustafaozen@harran.edu.tr

Russian translation published in *Mekhanika Kompozitnykh Materialov*, Vol. 52, No. 6, pp. 1081-1090, November-December, 2016. Original article submitted September 15, 2015; revision submitted May 14, 2016.

TABLE 1. Mechanical and Physical Properties of the Materials Used for Composites

Material	Density, kg/m ³	Elastic modulus, GPa	Tensile strength, MPa	Fiber diameter, μm
E-glass fiber	2500	70	1750	12
S-glass fiber	2600	90	4600	10
Carbon fiber	1500	220	3200	9
PVC foam	60	0.09	0.95	–
Epoxy resin	1100	3.1	75	–

Fabric structural composite products are usually made from different high-modulus fibers or yarns, such as glass, carbon, aramid, etc. ones. Each material has a particular advantage, for example, carbon exhibits the highest modulus or stiffness, but is lacking in toughness. On the other hand, glass fiber is the most dependable material for many textile composites due to its lower cost. Since each fiber type has a particular advantage, there have been extensive investigations into hybrid fiber composites, which are fabricated by combining two or more different reinforcement materials in a common matrix in a single composite system. By doing so, a new material is obtained with new and additional properties. As expected, the mechanical properties of the hybrid composites lie between those of single- fiber composites made of constituent fibers for the hybrid version [5, 6].

One of the major concerns in the use of a sandwich composite material is the damage induced in these materials by impacts of foreign objects, which are expected during the life of load-carrying structures. Impact-induced damage can reduce the stiffness of the structures and a residual strength occurs after the impact. For these reasons, the problem of impact on sandwich composite structures has received considerable attention in the literature [7-15]. The effects of various parameters, such as the impactor shape [16], weaving angles between interlacing yarns [17], hybridization [5, 6, 18, 19], temperature [20], and type of the core material [21, 22], on the drop-weight impact responses of composites have also been studied.

When composites are exposed to a low-speed impact, the resulting damage and the residual strength should be examined carefully. A decision has to be made whether the composite can continue to serve or it has to be replaced by a new one. Wang et al. [11] employed tensile tests after impact tests to determine the residual tensile strength of foam sandwich structures. Davies et al. [15] and Gustin et al. [23] employed compression tests after impact tests to determine the residual strength of the composites. Shim and Yang [24] employed four-point bending tests after impact tests to determine the residual mechanical properties of woven-carbon-fabric-reinforced composites.

The objective of this study was to investigate the effect of different stacking sequences of fabric layers in face sheets on the impact and postimpact bending behavior of hybrid sandwich composites. Impact and three-point bending tests were carried out to predict the peak load, deflection at the peak load for impact tests, and the flexural strength after impact loadings of hybrid composites.

2. Materials and Methods

2.1. Material preparation

Carbon, s-glass, and e-glass fabrics are plain-weave ones. The areal densities of carbon, s-glass, and e-glass fabrics employed were 300, 190, and 500 g/m², respectively. A bicomponent Araldite LY 564 epoxy resin with an Aradur 3487 BD hardener was selected as a thermoset polymeric matrix. The core for sandwich panels was a PVC foam of thickness 10 mm. The mechanical and physical properties of the materials used for the composites are given in Table 1. The composite sandwich laminates were fabricated by using a laboratory Vacuum-Assisted Resin Infusion Molding (VARIM) system and were cured for 8 h at 80°C. All configurations were produced using six fabric layers with a similar volume fraction and thickness and a core material. Six hybrid configurations were manufactured by arranging carbon, s-glass, and e-glass fabrics with different stacking sequences symmetrically to the core.

TABLE 2. Details of Test Specimens

Nomenclature	Number of specimens	Description
ESC	5	E-glass/s-glass/carbon/polythene-foam/carbon/s-glass/e-glass
ECS	5	E-glass/carbon/s-glass/polythene-foam/s-glass/carbon/e-glass
SCE	5	S-glass/carbon/e-glass/polythene-foam/e-glass/carbon/s-glass
SEC	5	S-glass/e-glass/carbon/polythene-foam/carbon/e-glass/s-glass
CSE	5	Carbon/s-glass/e-glass/polythene-foam/e-glass/s-glass/carbon
CES	5	Carbon/e-glass/s-glass/polythene-foam/s-glass/e-glass/carbon

2.2. Low-speed impact tests

Impact tests were performed by using a CEAST-Fractovis Plus instrumented drop-weight testing system with a hemispherical nose 12.7 mm in diameter. A piezoelectric load cell of capacity 22.4 kN was used in tests. All specimens were impacted with a 5-kg drop weight. Since the drop weight was not changed, the different impact energies were achieved by adjusting the drop height with a spring assist. A pneumatic clamping fixture with an opening 76.2 mm in diameter was used to fix each specimen during impact loading. Three different impact energies, equal to 7.5, 15, and 22.5 J, were used in this study. These energies were selected in order to assure that the impact did not result in full penetration of the laminate and that the extension of damage into a specimen did not exceed its width even under the highest energy applied. called A VisualIMPACT impulse software, to which the contact force between the impactor and specimen, impactor speed and energy, and the central deflection of test specimen as a function of time were given, was used to display and store impact data. The values of impact force were recorded at each time step by a data acquisition system (DAS).

2.3. Three-point bending tests

Three-point bending tests were performed on a Shimadzu Universal Tensile Machine with a 100-kN load cell for each configuration in accordance with ASTM D970-07. The specimens were tested in bending either after their production (non-impacted specimens) or after low-speed impact tests to measure their residual flexural strength. The flexural strength σ_f of the hybrid sandwich composites was calculated by the formula

$$\sigma_f = \frac{3PL}{2bd^2},$$

where L , b , d , and P are the support span, specimen width, specimen depth, and flexural load, respectively.

3. Results and Discussion

3.1. Impact properties

In the current study, specimens of dimensions 150 × 100 mm were tested at impact energies of 7.5, 15, and 22.5 J. All the hybrid sandwich composites prepared (see Table 2) were tested at each energy level.

Figures 1a-c shows load–deflection curves of the representative hybrid sandwich composites subjected to impact energies of 7.5, 15, and 22.5 J. For all impact energies, the slope of the ascending section (the bending stiffness) for all specimens was nearly the same, the peak load increased with impact energy, and a couple of oscillations were observed before the load

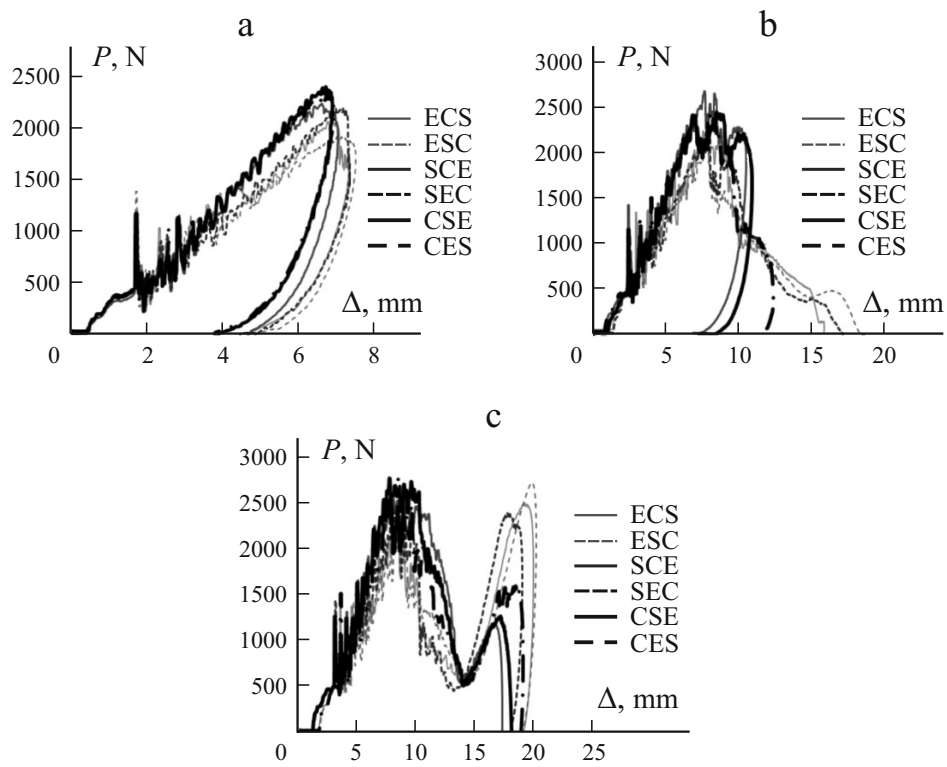


Fig. 1. Load vs. deflection curves P - Δ of representative hybrid sandwich composites at the impact energies of 7.5 (a), 15 (b), and 22.5 J (c).

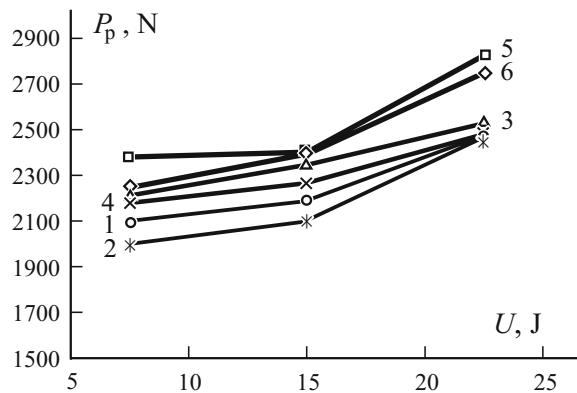


Fig. 2. Peak load P_p versus impact energy U : ECS (1), ESC (2), SCE (3), SEC (4), CSE (5), and CES (6).

reached the peak value, which pointed to a local failure of plies. There was a sudden drop in the load for all specimens when the load reached the peak value, which indicated that the top face of the sheet was perforated. Figure 1a shows load–deflection curves of the specimens subjected to the impact energy of 7.5 J. As seen in the Fig., all curves return back from the value of maximum load implying rebounding. As seen in Figs. 1b-c, except for the SCE and CSE specimens, the other curves do not return back, implying penetration of the impactor. In these cases, the load became zero at the end of the descending section. As seen in Fig. 1c, the curves are of a mountain-like shape with two peaks, implying the contact of impactor with the top and bottom face sheets. For the specimens subjected to the impact energy of 22.5 J, the value of the second peak load value was

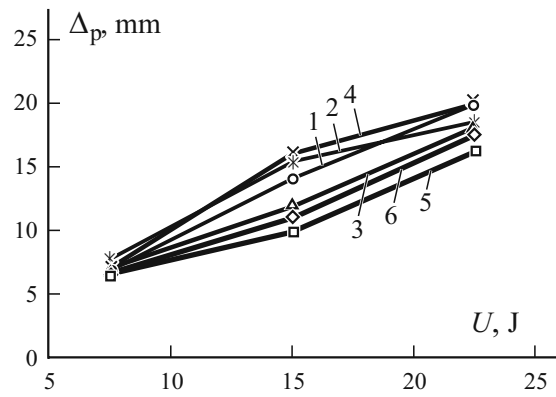


Fig. 3. Deflection Δ_p at the peak load versus impact energy U . Designations as in Fig. 2.

found to be nearly equal to the first one. The second peak corresponds to loading of the bottom face sheet. However, at the three levels of impact energy, the impactor did not penetrate the bottom face sheet.

Figure 2 illustrates the peak load P_p as a function of impact energy U . The threshold load for the peak loads seems to be around 2-2.9 kN for all the levels of impact energy used in the study. The peak loads for the hybrid sandwich composites with glass fabrics in face sheets were lower than those in the case of carbon fabrics for all energy levels. The peak loads increased roughly by 12.04, 8.28, and 14.19% at $U = 7.5$, 15, and 22.5 J, respectively, when carbon layers were in the top and bottom face sheets. The peak loads did not vary much within the range of impact energy levels used in this study.

Figure 3 illustrates the deflection Δ_p at the peak load P_p as a function of impact energy U . As seen, the deflection at the peak load increased with impact energy for all specimens. The deflection at the peak load of hybrid sandwich composites with e-glass and s-glass fabrics in face sheets was greater than that in the case of carbon fabrics for all the energy levels.

In low-speed impacts, the impact energy of impactor can be adjusted by changing the height of the drop load. When the impact energy and accordingly the impact speed increase, the impact/contact force also increases because of the growing momentum. The stress stiffening of face sheets and densification of the foam core also contribute to the increase in the contact force to some extent. It is well known that, up to the penetration of impactor into a specimen, the contact force increases with impact energy. Around the penetration point, the contact force generally reaches its peak value. At impact energies causing perforation, the contact force may decrease slightly. It should be noted that the specimens used in this study were not completely punctured at the levels of impact energy selected, that is, the back face sheets were not completely punctured in spite of perforation of the front/top face-sheets. At $U = 15$ J, the impactor was trapped in the target, while at $U = 22.5$ J, the target was punctured, which led to the emergence of a second peak on the contact curve. This second peak was inserted into the graphs in Fig. 2, showing the peak loads versus impact energies.

3.2. Postimpact flexural properties

As expected, the increase in the impact energy was caused by reduction in the flexural strength of the hybrid sandwich composites investigated. Figure 4 shows the flexural strength of undamaged and impact-damaged composites. As seen, the CSE hybrid sandwich composites had the highest flexural strength among the tested ones for all damage conditions. In contrary, the ESC hybrid sandwich composites had the lowest normal stress. Thus, the presence of carbon fibers in skin regions increased the flexural strength, but the presence of e-glass fibers decreased the strength. The hybrid composites with different stacking sequence of carbon, e-glass, and s-glass fibers showed differences in the resulting bending properties. Carbon fibers in skin regions were found to increase the flexural strength more than e-glass or s-glass one. In bending, the outermost layers bear most of the applied load, therefore, a high flexural strength was achieved when carbon fibers were located in skin regions. Similar results were obtained by Subagia et al. [25], who combined carbon fibers and basalt fabrics in different sequences.

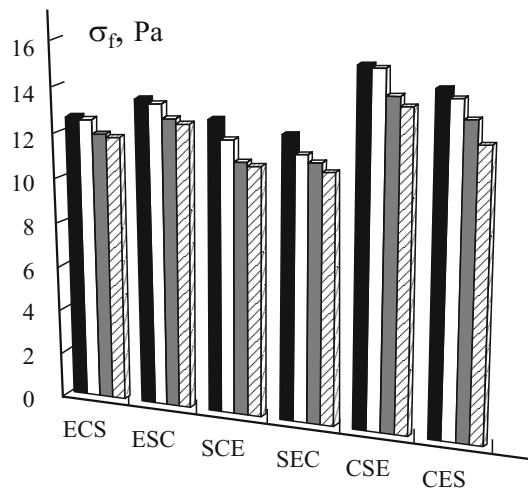


Fig. 4. Flexural strength σ_f of undamaged and impact-damaged composites at $U = 7.5$ (\square), 15 (\blacksquare), and 22.5 J (hatched).

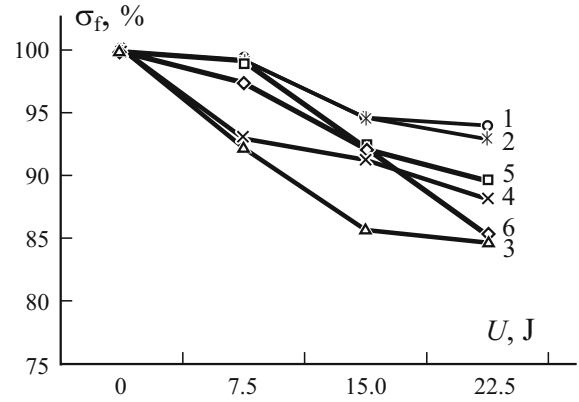


Fig. 5. The normalized flexural strength $\bar{\sigma}_f$ of nonimpacted and impacted specimens versus impact energy U : ECS (1), ESC (2), SCE (3), SEC (4), CSE (5), and CES (6).

In order to better evaluate the influence of impact energy on the flexural strength, the normalized flexural strength of each specimen was calculated as the ratio between the mean flexural strengths of nonimpacted and impacted specimens and shown in Fig. 5. As expected, all impact energies reduced the flexural strength of all configurations, but the effect of the 7.5-J impact was not significant. For the 7.5-J impact energy, the maximum reduction was observed for the SEC and SCE hybrids — 7 and 8%, respectively. It seems that, at low impact energies, placing s-glass fibers at skin regions showed the maximum reduction for the postimpact bending behavior. For the 15-J impact energy, a reduction in the flexural strength between 5 and 14% was observed for all configurations. The maximum reduction, equal to 14%, was found for the SCE laminates. The minimum reduction for the post-impact bending behavior, equal to 5%, was observed for the ECS and ESC configurations. In the case of e-glass fibers in skin regions, the reduction was minimum for the postimpact flexural strength at all impact energies. At the maximum impact energy, 22.5 J, the reduction in the flexural strength was between 6 and 15% for all configurations. The maximum reduction, equal to 15%, was observed for the CES and SCE configurations, while the minimum one, 6%, for the ECS configuration. For the hybrid composites with e-glass fibers in skin regions, impact loadings did not affect the flexural strength significantly. At the 7.5- and 15-J impact loadings, the maximum reduction was observed for the hybrids with s-glass fibers in skin regions, while at the 22.5-J impact loading, the reduction in strength for the CES configuration was greater than for the SEC one. Up to $U = 7.5$ J, all configurations showed a similar response to impact loadings, but the hybrid laminates with e-glass fibers in skin regions exhibit better postimpact properties. Thus, in impact loadings, the use of e-glass in skin regions showed more advantages than the employment of s-glass or carbon fibers.

4. Conclusion

Experimental investigations into the low-speed and postimpact bending response of hybrid sandwich composite panels composed of carbon/e-glass/s-glass fabrics as the reinforcement material, an epoxy resin as the matrix material, and a polythene foam as the core material have been carried out. The impact and postimpact bending data showed how the stacking sequence of carbon, s-glass, and e-glass fabrics affected the performance of the sandwich composites during and after impacts. The following conclusions were drawn from study.

For the impact response.

1. The peak loads for the hybrid sandwich composites with glass fabrics in face sheets were lower than those in the case of carbon fabrics at all the energy levels considered. They increased roughly by 12.04, 8.28, and 14.19% at $U = 7.5$, 15, and 22.5 J, respectively, when carbon layers were in the top and bottom face sheets.

2. At peak loads, deflections of the hybrid sandwich composites with e-glass and s-glass fabrics in face sheets were higher than for those with carbon fabrics at all the energy levels considered.

3. Carbon fibers in skin regions were found to increase the flexural strength more than an e-glass or s-glass layer in these regions.

For the post impact bending response.

1. All impact energies reduced the flexural strength for all configurations, but the 7.5-J impact did not affect the flexural strength significantly.

2. After a 7.5-J impact, the maximum reductions in the flexural strength were observed for the SEC and SCE hybrids, 7 and 8%, respectively.

3. After a 15-J impact, a reduction in the flexural strength between 5 and 14 was observed for all configurations. The maximum reduction, 14%, was for the SCE laminates. The minimum reductions, 5%, for the postimpact bending behavior was observed for the ECS and ESC configurations.

4. After a 22.5-J impact, a reduction in the flexural strength between 6 and 15% was observed for all configurations. The maximum reductions, 15%, were revealed for the CES and SCE configurations, but the minimum reduction, 6%, was found for the ECS configuration.

5. The hybrid composites with e-glass fibers in skin regions showed a better performance than the s-glass and carbon fibers in the regions at all energy levels for the postimpact response and exhibited greater displacements, therefore having a lower load-carrying ability than the other hybrid laminates.

As a result, for the hybrid sandwich configurations considered in this study, we can conclude the following.

I. The composites with a carbon reinforcement in the uppermost and lowermost layers had the highest bending stiffness.

II. With increasing impact energy, the lowest reduction rate for the residual bending strength was observed in the case of e-glass fabrics in the uppermost and lowermost layers of the ECS and ESC configurations when the stacking sequences were considered individually. However, when they were considered together, the CES and CSE ones had the highest values of the residual bending strength.

REFERENCES

1. R. Ferri and B. V. Sankar, "Static indentation and low-velocity impact test on sandwich plates," *Proc. of the ASME Aerospace Division*, **55**, (1997), pp. 485-490.
2. J. Xiong, L. Ma, L. Z. Wu, J. Y. Liu, and A. Vaziri, "Mechanical behavior and failure of composite pyramidal truss core sandwich columns," *Compos. Part B-Eng.*, **42**, 938-945 (2011).
3. K. Finnegan, G. Kooistra, H. N. G. Wadley, and V.S. Deshpande, "The compressive response of carbon fiber composite pyramidal truss sandwich cores," *Int. J. Mater. Res.*, **98**, 1264-1272 (2007).
4. T. S. Lim, C. S. Lee, and D. G. Lee, "Failure modes of foam core sandwich beams under static and impact loads," *J. Compos. Mat.*, **38**, 1639-1662 (2004).
5. T. Anderson and E. Madenci, "Experimental investigation of low velocity impact characteristics of sandwich composites," *Compos. Struct.*, **50**, 239-247 (2000).
6. E. Sevkat, B. Liaw, F. Delale, and B. B. Raju, "Drop-weight impact of plain-woven hybrid glass-graphite/toughened epoxy composites," *Compos. Part A-Appl.*, **40**, 1090-1110 (2009).
7. G. B. Chai and S. Zhu, "A review of low-velocity impact on sandwich structures," *J. Materials Des. Appl.*, **225**, 207-230 (2011).

8. J. Kepler, "Impact penetration of sandwich panels at different velocities — an experimental parameter study: Part II — interpretation of results and modeling," *J. Sandw. Struct. Mater.*, **6**, 379-397 (2004).
9. S. Feli and M. Namdari, "An analytical model for composite sandwich panels with honeycomb core subjected to high velocity impact," *Compos. Part B-Eng.*, **43**, 2439-2447 (2012).
10. S. Bartus and U. Vaidya, "A review: impact damage of composite materials," *J. Adv. Mater.*, **39**, 3-21 (2007).
11. B. Wang, L. Z. Wu, L. Ma, and J. C. Feng, "Low-velocity impact characteristics and residual tensile strength of carbon fiber composite lattice core sandwich structures," *Compos. Part B-Eng.*, **42**, 891-897 (2011).
12. M. S. Patrick, J. J. Luo, and I. M. Daniel, "Low-velocity impact behavior of composite sandwich panels," *Compos. Part A-Appl.*, **36**, 1389-1396 (2005).
13. K. B. Shin, J. Y. Lee, and S. H. Cho, "An experimental study of low-velocity impact responses of sandwich panels for Korean low floor bus," *Compos. Struct.*, **84**, 228-240 (2008).
14. T. Anderson and E. Madenci, "Experimental investigation of low-velocity impact characteristics of sandwich composites," *Compos. Struct.*, **50**, 239-247 (2000).
15. J. Gustin, A. Joneson, M. Mahinfallah, and J. Stone, "Low-velocity of combination Kevlar/carbon fiber sandwich composites," *Compos. Struct.*, **69**, 396-406 (2005).
16. K. M. Fard, S. M. R. Khalili, S.H. Forooghi, and M. Hosseini, "Low-velocity transverse impact response of a sandwich plate subjected to a rigid blunted cylindrical impactor," *Compos. Part B-Eng.*, **63**, 111-122 (2014).
17. C. Atas and D. Liu, "Impact response of woven composites with small weaving angles," *Int. J. Impact Eng.*, **35**, 80-97 (2008).
18. M. V. Hosur, M. Abdullah, and S. Jeelani, "Manufacturing and low-velocity impact characterization of hollow integrated core sandwich composites with hybrid face sheets," *Compos. Struct.*, **65**, 103-115 (2004).
19. M. V. Hosur, M. Abdullah, and S. Jeelani, "Manufacturing and low-velocity impact characterization of foam filled 3-D core sandwich composites with hybrid face sheets," *Compos. Struct.*, **69**, 167-181 (2005).
20. J. Liu, X. Zhu, T. Li, Z. Zhou, L. Wu, and L. Ma, "Experimental study on the low-velocity impact responses of all-composite pyramidal truss core sandwich panel after high temperature exposure," *Compos. Struct.*, **116**, 670-681 (2014).
21. M. Meo, R. Vignjevic, and G. Marengo, "The response of honeycomb panels under low-velocity impact loading," *Int. J. Mech. Sci.*, **47**, 1301-1325 (2005).
22. C. Atas and C. Sevim, "On the impact response of sandwich composites with cores of balsa wood and PVC foam," *Compos. Struct.*, **93**, 40-48 (2010).
23. G. A. O. Davies, D. Hitchings, and G. Zho, "Impact damage and residual strengths of woven fabric glass/polyester laminates," *Compos. Part A-Appl.*, **27**, 1147-1156 (1996).
24. V. P. W. Shim and L. M. Yang, "Characterization of the residual mechanical properties of woven fabric reinforced composites after low-velocity impact," *Int. J. Mech. Sci.*, **47**, 647-665 (2005).
25. I. D. G. A. Subagia, Y. Kim, L. D. Tijjing, C. S. Kim, and H. K. Shon, "Effect of stacking sequence on the flexural properties of hybrid composites reinforced with carbon and basalt fibers," *Compos. Part B-Eng.*, **58**, 251-258 (2014).